Journal of Applied Fluid Mechanics, Vol. 15, No. 3, pp. 757-765, 2022.
Available online at www.jafmonline.net, ISSN 1735-3572, EISSN 1735-3645.
https://doi.org/10.47176/jafm.15.03.33149

Experimental Study on Breakup and Transition of a Rotating Liquid Jet

C. K. Chen[1], C. C. Chang[2], W. M. Yan[3,4], W. K. Li[5†] and T. H. Lin[1,2]

[1] *Research Center for Energy Technology and Strategy, National Cheng Kung University, Tainan 70101, Taiwan*
[2] *Department of Mechanical Engineering, National Cheng Kung University, Tainan 70101, Taiwan*
[3] *Research Center of Energy Conservation for New Generation of Residential, Commercial, and Industrial Sectors, National Taipei University of Technology, Taipei 10608, Taiwan*
[4] *Department of Energy and Refrigerating Air-Conditioning Engineering, National Taipei University of Technology, Taipei 10608, Taiwan*
[5] *Department of Mechanical Engineering, Chung Yuan Christian University, Taoyuan 32023, Taiwan*

†*Corresponding Author Email: g990401@gmail.com*

(Received July 3, 2021; accepted December 20, 2021)

ABSTRACT

The present study pertains to the experimental work on the characteristic of a rotating liquid jet under various conditions of the nozzle diameter, volumetric flow rate and rotating speed. With emphasis on the important phenomena of a liquid jet, the effects of breakup length, the transition between dripping and jetting, breakup categories, droplet sizes from the breakup, and the time interval between two successive droplets are investigated systematically. The results reveal that the breakup length of a jet increases with flow rate and decreases with imposed rotation. The hysteresis behavior only occurs for larger nozzles, and the transition from jetting to dripping is affected by the imposed rotation. Depending on the imposed rotation, three different breakup patterns are found and named single droplet, satellite droplet, and multi-position necking. An empirical correlation is also proposed to predict the boundary of satellite and multi-droplets formation. The main droplet, satellite droplet, and merged droplet are about 1.8, 0.8, and 2.2 times than the nozzle diameters, respectively, no matter what the rotating speed is. Moreover, the non-dimensional time interval between two main droplets has an ascending tendency with either We number or the imposed rotation.

Keywords: Rotating speed; Breakup length; Transition; Hysteresis behavior.

NOMENCLATURE

D	droplet size
d_j	unperturbed diameter of a jet
DJ	dripping to jetting
JD	jetting to dripping
L	Hocking parameter
L_j	breakup length of a jet
$\dot{Q}$	flow rate
Re	Reynold number, $Re = \rho V d_j/\mu$
RLC	rotating liquid column
RLJ	unperturbed radius of a jet
T	time interval
T^*	non-dimensional time interval
V	jet velocity
We	Weber number, $We = \rho V^2 d_j/\sigma$
σ	surface tension
μ	viscosity
ρ	density
ω	Rotating speed
χ	swirl parameter, $\chi = r\omega/V$

1. INTRODUCTION

The characterizing of the liquid jet breakup to form a droplet is an extremely important phenomenon either in daily life or in industrial application (Tang *et al.* 2021). With increasing industrial interest, the disintegration of a liquid jet into droplets increases not only the surface area but also the mass and heat transfer (Chemloul 2012; Morad *et al.* 2020), which is used widely in spray cooling (Krištof *et al.* 2019; Labergue *et al.* 2015), 3D printing (Gao and Zhou 2019), injector (Chung *et al.* 2015; Ghate *et al.* 2019), and drug delivery device (Bonhoeffer *et al.* 2017; Brandau 2002). By properly understanding the breakup of a liquid jet, characteristics of the

breakup length, droplet formation, and transition point between dripping and jetting are essential in optimizing the system performance.

The earliest quantitative investigation on the behavior of liquid jets was done by Savart (1883), observing the mutual relation between jet velocity and jet integration, and systematically examining the decay of a liquid jet, thereafter called "instability". Rayleigh (1879) proposed the theoretical analysis on the mechanism of jet breakup by considering the effect of surface tension, and developed a jet instability model. The linear theory indicated that the growth rate of a jet grew with time exponentially and breakup occurred simply when the disturbance grew to the equal level of the jet radius. Systematic estimation of the drop size is another crucial factor to understand the behavior of a jet. Ashgriz and Mashayek (1995) predicted the droplet size based on the wavelength of the most unstable wave of a jet, which refers to the natural breakup point. In the past decades, a number of works have been devoted to the instability phenomenon of the jet breakup theoretically (Bogy 1979; Y. b. Wang *et al.* 2018; Yang *et al.* 2017), experimentally (Clanet and Lasheras 1999; Son and Ohba 1998; F. Wang and Fang 2015) and numerically (Amini *et al.* 2013). In addition, comprehensive reviews of this subject are available to study the historical development and the underlying physical mechanisms, e.g., McCarthy and Molloy (1974), UTREJA and HARMON (1990), and Birouk and Lekic (2009).

Relatively, less attention was paid to the physical behavior of the rotating liquid jet (RLJ) or rotating liquid column (RLC). Understanding the dynamics of rotating jets, including instability mechanisms, droplet formations, and the factors affecting the distribution of their sizes, is increasingly important (Li *et al.* 2019). It is inevitable to observe the more complex dynamics involved in the rotating jet instability compared with non-rotating one. Hocking and Michael (1959) considered the stability of a long rotating liquid jet being affected by plane disturbances and introduced the Hocking parameter, $L=\sigma/\rho\omega^2 r_j^3$, to examine instability sources which were the fluid rotation and shear across the region with different angular velocities. Afterwards, Gillis (1961) took viscosity into account, investigating the effect of fluid viscosity on the stability of a spinning jet. He discovered theoretically that viscosity could not destroy the stability of a system. Therefore, the force equilibrium should be balanced between surface tension and centrifugal force. Rutland and Jameson (1970) solved the linear instability of RLC by assuming the perturbation was in a form of sinusoidal wave. Although they developed the outstanding equations for describing the growth rate of RLC, the experiment data still showed a scattered agreement with theoretical prediction.

Eggers and Brenner (2000) presented a numerical study which described the changes of angular momentum of a rotating jet in radial direction. It was clear that the centrifugal forces became bigger when the radius of RLC went to zero. They also indicated that the angular momentum of a jet would be expelled rapidly near the pinching region and concentrated in the center. Zahniser (2004) investigated the behavior of a rotating water jet, and separated the various forms of stability. If the rotating speed increased gradually, the jet broke down into two-lobed, bar shaped forms. His inequality prediction provided a quick method to identify the dominant mode of RLC. Kubitschek and Weidman (2007a) developed their perturbation theory and thus proved that the rotation would drastically affect the growth rate and the most unstable wavenumber under the circumstance of Hocking parameter $L < 0.1$; namely the rotation should be large enough to exceed that critical point or the outcome of rotation on both growth rate and wavenumber would not be observed. The same team of Kubitschek and Weidman (2007b) presented that the preferred RLC mode boundaries compensated the inequality and the mode diagram with viscosity was set to find out the pattern of RLC. Weidman *et al.* (2008) further studied the shape of rotating jet and granular flow. They found that the momentum model showed the 0.866 rj contraction of jet radius for when a jet is issued from the horizontal tube and the swirl parameter, χ, is a critical factor for the reduction of the jet contraction. Li *et al.* (2019) studied the generation of drops by spiralling liquid jets with focuses with the formation of drops and satellite droplets emitted from the end of the jet. Lu *et al.* (2020) proposed a rotating jet impingement cooling system to evaluate its performance by numerical simulations. Effects of the governing parameters, such as the jet exit Reynolds number, rotation speed, and coolant physical properties on the heat transfer are investigated. One correlation based on the rotation speed, average Nusselt number, Reynolds number and were also developed.

Despite more than one century of continuing efforts, the mechanisms of the breakup and transition of a liquid jet are still far from being completely elucidated, from an extensive literature survey. Although Rutland and Jameson (1970) proved that rotation had great influence on a jet, the jet in their experiment was vibrated and viscous. Therefore, the investigation of the rotation effect on a natural jet still remains unsolved. Furthermore, the transition point for RLC has not yet been studied in detail and, thus, the mutual relation between dripping and jetting is vigorously surveyed in this study as well. The objective of the work is dedicated to analyzing the rotating liquid jet with focuses on the effects of various conditions, such as the nozzle diameter, volumetric flow rate and rotating speed, on the breakup length, the transition between dripping and jetting, breakup patterns, droplet sizes from the breakup, etc.

2. EXPERIMENTAL SETUP AND MEASUREMENT

The aim of the experiment is to investigate the behavior of the RLJ under various circumstance, e.g., the effect of exit velocity, the influence of the

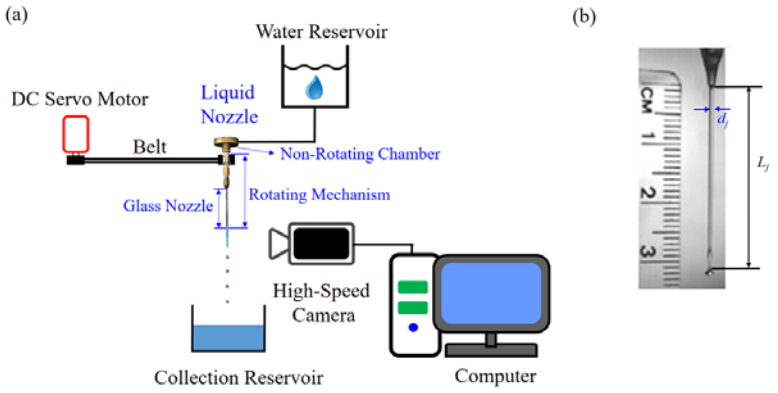

Fig. 1. Schematic of the (a) experimental setup and (b) jet breakup length.

imposed rotation and so on. Hence, the equipment in this study should be capable of controlling flow rates, making a nozzle rotate about its axis, and recording a series of consecutive images. The precise measurement is also desperately needed for further analysis; thus, a tachometer plays an important role in confirming the rotation rate.

The experimental setup and the constituent apparatus are displayed in Fig. 1(a). The water reservoir is fixed on the top of an extendable steel rod and connected to the upper part of the liquid nozzle with a plastic tube. As shown in Fig. 2, a liquid nozzle system can be divided into a non-rotating chamber and a rotating mechanism. After the fluid flows from the reservoir via the plastic tube, the fluid is piling up in the non-rotating chamber of the upper part of the liquid nozzle. Then, the fluid is able to flow into the rotating mechanism which is composed of two parts as below. The first part consists of a roller bearing and two joint shaft pins at both ends, located in the middle of the entire nozzle system. The second part is basically the glass nozzle itself and the nozzle diameter is changeable to be easily adjusted to meet the experimental condition.

As for the rotation transmitting mechanism, the DC servo motor is used for modulating the rotating speed. The shaft of the motor is fixed at the center of the downward roller bearing, which is connected to the other roller bearing with belt. In order to make a jet rotate, the rotating mechanism of a nozzle should be inserted into the roller bearing. Though the rotation rate can be observed easily by the images captured by the high-speed camera, we also utilize a tachometer for double checking the rotation rate generated by the motor. The high-speed camera used in this study captures images at the rate of 15000 to 20000 pictures within a second, which is enough to observe the clear dynamical interaction of liquid jet breakup. The experimental images are recorded into a computer for further image-cropping or grey level transformation by using the programming software of MATLAB. The size of the droplet is predicted from these images based on the wavelength of the most unstable wave of a jet, which refers to the natural breakup point.

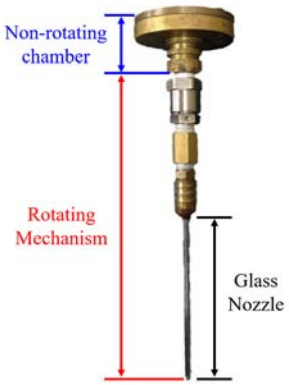

Fig. 2. Diagram of the liquid nozzle System.

Following the description of the breakup length of a jet suggested by former researcher, Chandrasekhar (1961), the intact length, denoted as L_j, is from the exit of nozzle to the position where the droplet starts to detach from the main jet as shown in Fig. 1(b) for the schematic of the definition of breakup length (L_j) and unperturbed jet diameter (also referred as the nozzle diameter) of d_j. As a matter of fact, the breakup length of a natural jet is not steady, that is, the length varies from time to time. Since the deviation between each case is not too large, we take an average value of the breakup length from at least 25 pinching images. Moreover, the breakup time is defined as the time interval which starts from the detachment of the main droplet to the next one.

3. RESULTS AND DISCUSSION

In this section, experimental results of rotating jets are discussed thoroughly. At first, the mode of RLJ is introduced, using the definition provided by Kubitschek and Weidman (2007a). Referring to the Hocking parameter L, defined as $\sigma/\rho\omega^2 r_j^3$, and the rotating Re_ω number ($r_j^2\omega/\nu$), a rotating jet in either axisymmetric or spiral mode can be determined based upon the flow condition. As observed in Fig. 3, the maximum operating parameters (ω = 1000 rpm in d_j = 1500 μm) in this study are L = 10.94 and Re_ω = 0.28, which are far from the boundary

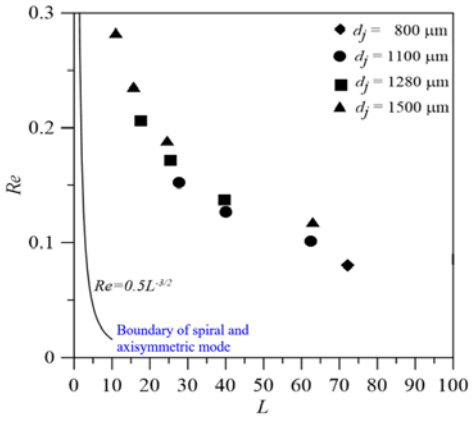

Fig. 3. Axisymmetric mode of rotating liquid jet used in this study.

between spiral and axisymmetric modes, and the values indicate that the whole experimental process keeps the jet perturbed axisymmetrically.

3.1 Breakup length of the RLJ

Figures 4 and 5 show the breakup lengths of the rotating jets over different flow rates and *We* numbers, respectively, for six different nozzles at four rotating speeds, i.e. ω = 0, 500, 800, and 1000 rpm. The red solid line denotes the theoretical results of Grant and Middleman (1966), which shows reasonable agreement with our experimental data. The breakup length of a jet becomes longer as the flow rate increases, resulting from the fact that the enhanced inertia forces in gravitational direction have more momentum to build an intact column. For the cases of ω= 0rpm, a vital phenomenon called "hysteresis" is observed for bigger nozzles with d_j = 1100, 1280, and 1500 μm, plotted in black and dashed lines. This hysteresis phenomenon is found by adjusting the flow rate in the transition zone either from dripping to jetting (DJ) or from jetting to dripping (JD). For the case of the DJ, after the fluid flows out of the nozzle, part of the fluid will be accumulated around the orifice and the surface tension forces become a significant barrier which makes the flow hard to exit, leading the hysteresis behavior. However, the surface tension forces are not the majority to be considered in the case of JD, and the disturbances from the surrounding are crucial instead.

As presented in Fig. 4(f) for d_j = 1500 μm, the hysteresis region is marked from 0.72 to 0.82 ml/s, implying that the critical flow rate of the transition from dripping to jetting (denoted as DJ) of 0.82 ml/s is different to that from jetting to dripping (denoted as JD) of 0.72 ml/s.

If an imposed rotation is exerted on the jet, it is obvious that the breakup length becomes shortened because of the extra disturbance. For example, comparing the corresponding breakup length in d_j = 550 μm at $\dot{Q}$ = 0.5 ml/s under ω = 0 rpm and 500 rpm as shown in Fig. 4(a), and the results can be found as 52 and 33 mm, respectively. For the larger nozzles, d_j = 1100, 1280, 1500 μm, the breakup

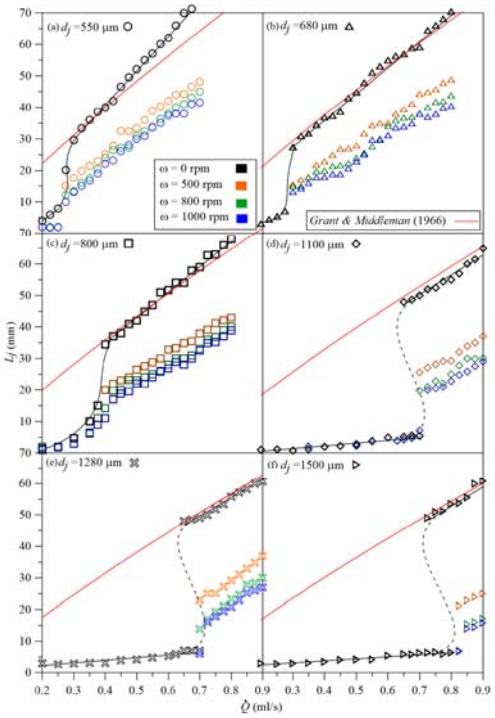

Fig. 4. Breakup length of rotating jets at different flow rates.

lengths at ω = 800 and 1000 rpm tend to be similar to each other and are quite lower than the ones at ω = 500 rpm as shown in Figs. 4(d) to 4(f). Furthermore, at a same rotating speed which is applied to each case, e.g., ω = 500 rpm, the breakup length is much shorter for the larger nozzle diameter. This phenomenon could be well explained by introducing the swirl parameter $\chi = r\omega/V$, which is the ratio of tangential velocity to exit velocity. The tangential velocity is enhanced with an increase in the nozzle diameter, leading to the reduction in the breakup length of a jet.

In Fig. 5, it is apparent that all the experimental data at each rotating speed lie on an ascending line, that is to say, if we impose an identical rotation on a jet in different nozzles, the outcomes of the non-dimensional breakup lengths tend to be restricted on a line with certain slope. Also, the rotating speed will change the slope value of this characteristic curve; specifically, the slope of this breakup curve decreases as the rotating speed is enhanced. For example, the slope at ω = 500 rpm is around 1.81, whereas the slopes are respectively about 1.28 at ω = 800 rpm and 1.09 at ω = 1000 rpm through linear fitting. Consequently, the experimental result discloses that the characteristics of the breakup length of a rotating jet follow a certain regulation under an arbitrary rotating speed.

3.2 Transition point

As discussed in the previous subsection, it is obvious that the imposed rotation has a great

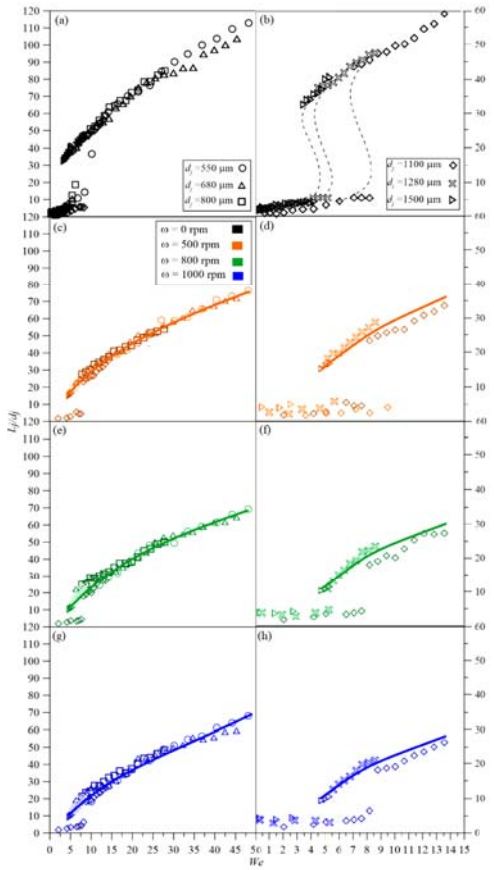

Fig. 5. Breakup length of rotating jets at different rotating speeds for various nozzle diameters.

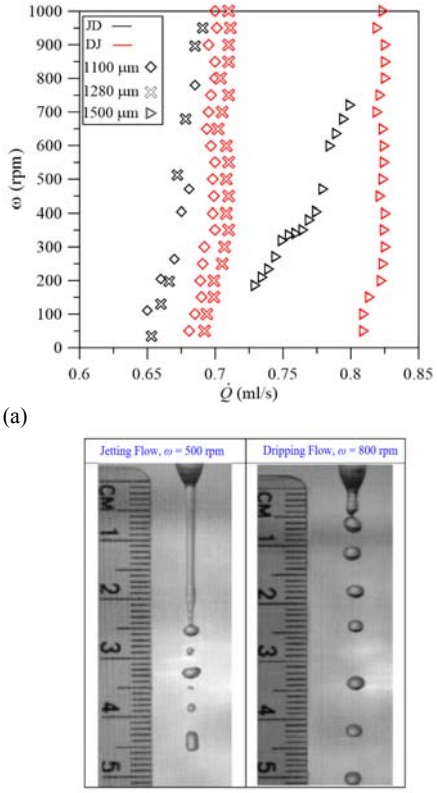

Fig. 6. (a) Transition points of rotating jets for DJ and JD cases, and (b) demonstration of the rotating effect on transition point with d_j = 1100 μm and $\dot{Q}$ = 0.68 ml/s.

influence on the jet breakup. Therefore, the following discussion focuses on the effect of rotation on the transition in DJ and JD cases. Figure 6(a) shows the transition interval when a rotation is imposed on a jet in bigger nozzles, *i.e.* d_j = 1100, 1280, 1500 μm. There are no transitions in small nozzles because the hysteresis behavior does not occur. Thus, only nozzles with hysteresis behavior are discussed on the transformation of the transition interval.

Firstly, the flow from JD is discussed to realize the influence of rotation. As seen in Fig. 6(a), the JD transition at the flow rate of $\dot{Q}$= 0.75 ml/s in d_j = 1500 μm occurs when the imposed rotation reaches 315 rpm. In the case of d_j = 1100 μm, a jetting flow decreases to 0.675 ml/s, and then, a 400 rpm rotation is required to make the jet start to drip. This is attributed to the reason that a huger liquid column generated by a large nozzle diameter requires a higher flow rate to form the breakup droplets. Besides, the critical rotating speed is approximately linear proportional to flow rate, which means that the critical rotating speed increases with the increasing flow rate. The detailed images can be referred to Fig. 6 (b), which demonstrates a jet at the same flow rate of 0.68 ml/s but at different conditions of rotating speed, resulting in jetting flow and dripping flow, respectively. Then, for the DJ case, $\dot{Q}$ = 0.7 ml/s is the critical flow rate for a dripping flow at 400 rpm in d_j = 1100 μm. Hence, it is apparent that the critical flow rate of a rotating dripping flow seems to be fixed, which means that the critical flow rate in DJ case stays the same no matter if the rotation is imposed. As a result, the rotation does not have any influence on DJ cases, whereas it does have severe effect on JD cases.

3.3 Breakup categories

The droplet formation could be categorized into three patterns as single droplet (also includes dripping flow), satellite droplet, multi-position necking, referring to pattern (a), pattern (b), and pattern (c), respectively. Figure 7 presents the breakup patterns of a rotating jet at ω = 500, 800, and 1000 rpm. Due to the absence of hysteresis behavior in smaller nozzles, it becomes clear to clarify the influence of rotation on breakup categories. The JD and DJ cases are plotted separately on left and right hand sides. As shown in Fig. 7, we can find that single droplet formation, called pattern (a), is quite rare while the rotation is imposed in smaller nozzles at low flow rates. Enhancing the rotation speed changes the breakup pattern from pattern (b), satellite droplets, to pattern (c), multi-position necking. Moreover, multi-positions necking, i.e. pattern (c), tends to occur in

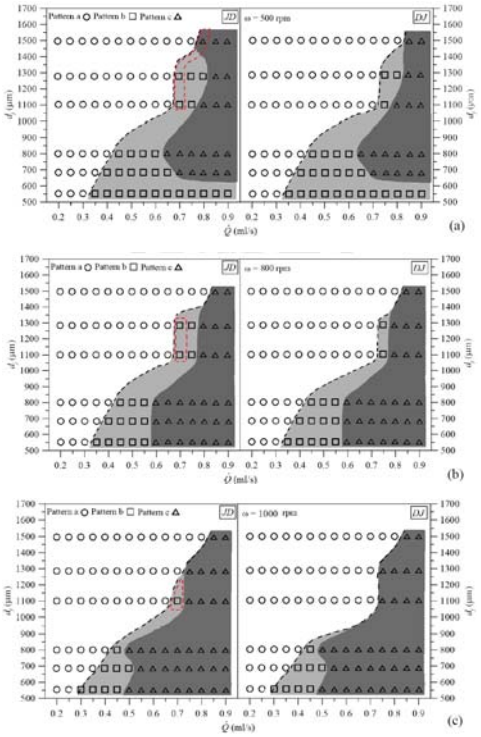

Fig. 7. Breakup patterns at (a) ω = 500 rpm; (b) ω = 800 rpm; (c) ω = 1000 rpm.

larger flow rate with higher rotating speed because the shear forces exerted on jet surface become more drastic as the inertia energy increases, resulting in the enhancement in surface perturbation to create multi-position necking droplets. The black contour expands with the increase in rotating speed, which means that pattern (b) in this case is replaced by pattern (c). For larger nozzles, the patterns are more complex due to the occurrence of hysteresis. It is found that pattern (c) becomes dominant as rotating speed increases, leading to an influential disturbance on the jet. The red dashed line represents the hysteresis region, and pattern (a) of DJ is substituted for pattern (b) or pattern (c) in the region of JD. Furthermore, there are some changes in JD patterns owing to the critical rotating speed; for example, with the comparison with conditions of ω = 500 and 800 rpm, the droplet formation of pattern (c) at $\dot{Q}$ = 0.8 ml/s in d_j = 1500 μm transforms directly into pattern (a), dripping flow, because the rotating speed exceeds its critical value.

Figure 8 shows the breakup categories in non-dimensional form. As a flow is in low *We* number region leading to a short liquid column, high swirl parameter χ is required to increase the amplitude of disturbances and transform the satellite droplet formation into multi-positions necking. By contrast, low swirl parameter χ is enough to transform the satellite droplets formation into multi-positions necking while a flow is in high We number region. To explain this phenomenon, we should first realize that any kind of forces would be treated as disturbances in jet formation, and, in turn, the

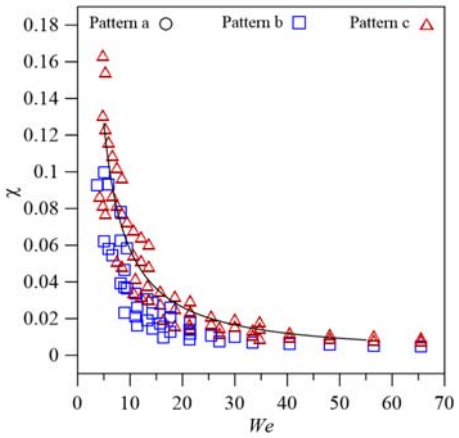

Fig. 8. Nondimensional rotating breakup patterns.

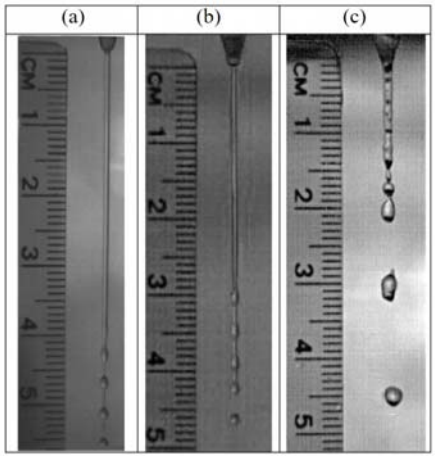

(a) Two positions necking
d_j= 800 μm; $\dot{Q}$= 0.7 ml/s; ω = 0 rpm.
(b) Three positions necking
d_j= 800 μm; $\dot{Q}$ = 0.7 ml/s; ω = 500 rpm.
(c) Drastic-perturbed necking
d_j= 1100 μm; $\dot{Q}$= 0.75 ml/s; ω= 1000 rpm.

Fig. 9. Different mechanisms of multi-position breakup.

tangential energy and inertia energy will compensate with each other to meet the minimum threshold for pattern (c) to occur. The fitting curve in Fig. 8 is collected by the average data points of pattern (c), and it can be expressed as

$$\chi = 0.78We^{-1.1} \tag{1}$$

The above empirical correlation can be treated as a boundary that separates the pattern of satellite formation and multi-position necking. Hence, it can be found that pattern (b) occurs when the experimental parameter is operated beneath this curve. Last but not least, Fig. 9 gives us a clear example of the difference in pattern (c) which is caused only by inertia forces as Fig. 9(a), rotation in Fig. 9(b), and high speed rotation (Fig. 9(c)). The

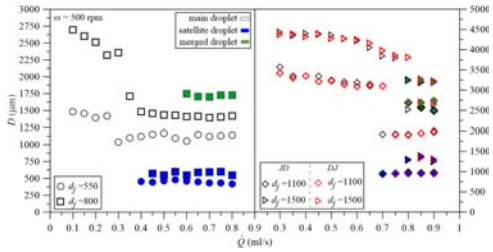

(a)

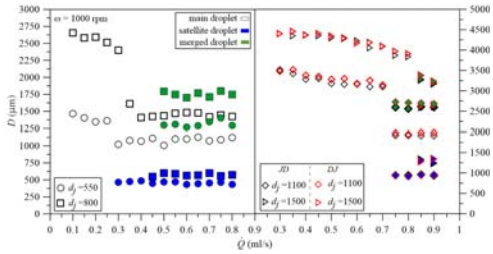

(b)

Fig. 10. Sizes of detached and breakup droplets at (a) ω= 500 rpm and (b) ω= 1000 rpm.

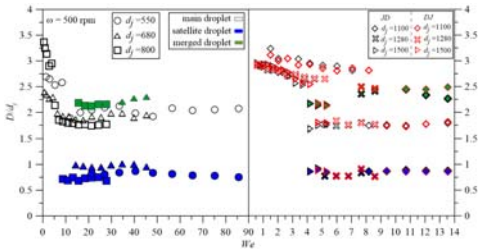

(a)

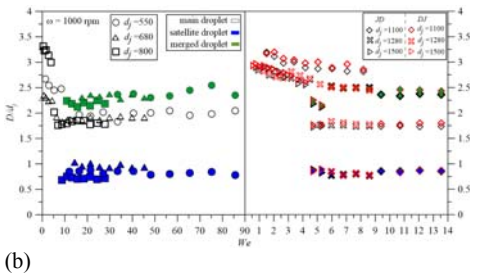

(b)

Fig. 11. Non-dimensional Sizes of detached and breakup droplets at (a) ω= 500 rpm and (b) ω= 1000 rpm.

difference in Figs. 9(a) and 9(b) is that there are two pinch points at most in a natural jet with ω = 500 rpm, whereas there can be three pinch points at maximum in a rotating jet ω = 800 rpm. It is because a natural jet is only perturbed by inertia forces, but a rotating jet is perturbed by both inertia forces and tangential forces, and thus, three positions necking can be expected.

3.4 Drop size from the breakup of the RLJ

The sizes of detached and breakdown droplets from various nozzle diameters are plotted with various flow rates at ω = 500 and 1000 rpm in Fig. 10. The large nozzles are plotted in the right part of this figure to emphasize the behavior of hysteresis. The sizes of detached droplets in dripping flow is in reverse proportion to flow rate since surface tension forces are fully responsible for the droplets in dripping flow. The energy is consumed faster while the inertia energy increases, leading to the early detachment and smaller size of the droplet. Moreover, it is obvious that there are sudden jumps around transition points. For d_j = 800 μm, one can expect the jump occurs at 0.35 ml/s at either ω = 500 rpm or 1000 rpm. As a result, the imposed rotation has minor influence on the droplet sizes. In the case of d_j = 550 μm, the sizes of main droplets are around 1050 μm at both ω = 500 and 1000 rpm. The effect of the imposed rotation on sizes of merged and satellite droplets is not obvious. Thus, we may conclude the imposed rotation has little effect on droplet sizes, but changes the breakup pattern.

It will be more clearly to clarify the relationship between flow rate and droplet size in standardized parameter. The non-dimensional droplet sizes with *We* number are displayed in Fig. 11, as expected, the main droplets which break down from different nozzles seem to remain at 1.8 times as bigger as the nozzle diameters at both ω = 500 and 1000 rpm, indicated in black hollow symbols. And the satellite droplets also stay at 0.8 times smaller than their corresponding nozzle diameters as denoted by blue solid symbols. However, the sizes of merged droplets are approximately 2.2 to 2.3 times bigger than their own nozzle diameters.

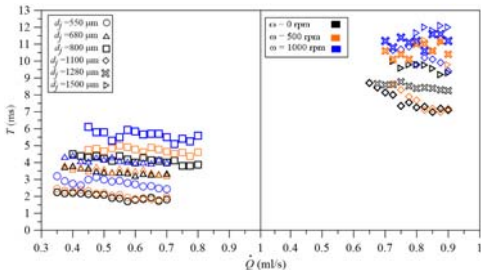

Fig. 12. Time interval of the rotating jets.

3.5 Time interval of the breakup of RLJ

The time interval between two main droplets is also of interest since it stands for the natural period of the breakup behavior. Figure 12 shows the breakup interval of main droplets in various nozzles, and it is separated into two parts: the experimental data from small nozzles on the left hand side and those from large nozzles on the right. The breakup interval increases with the increasing rotating speed, indicating that it takes slightly longer to break a main droplet from the liquid column. However, it is important to note that the breakup interval is not definitely increased when the rotation is imposed. This makes the breakup become chaotic and thus the observed time interval starts to be scattered, and, hence, the best way to show the influence of rotation is by plotting the range of time interval.

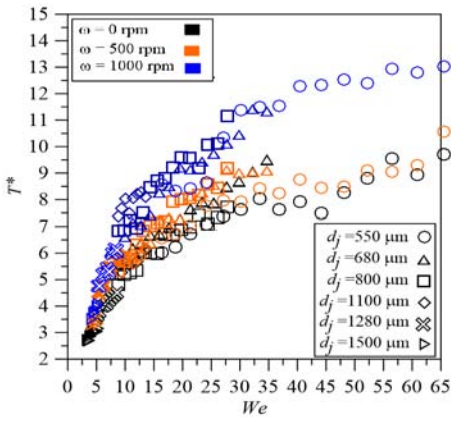

Fig. 13. Non-dimensional time interval of the rotating jets.

Besides, it is understandable that the time interval increases since the breakup length is much shorter when a rotation is imposed. In the right part of Fig. 12, the time intervals of larger nozzles are not stable, apparent fluctuation of time, as that in smaller nozzles, and the effect of rotation is easy to be observed.

Figure 13 shows the non-dimensional time interval of different rotating speed and nozzles. As plotted in this figure, the rotating time interval has a similar pattern as that at ω = 0 rpm, which can be seen as a hyperbolic curve. There are a lot of ω = 500 rpm experimental data overlapped with ω = 0 rpm, suggesting the tangential forces is not strong enough to affect the characteristic curve of rotating time interval.

4. CONCLUDING REMARKS

In the present work, the characteristic of a rotating liquid jet under various conditions, such as nozzle diameter, flow rate and rotating speed, is studied experimentally. Based on the results above, the following conclusions can be drawn.

1. Enhancing the flow rate increases the breakup length of a jet, but the breakup length is reduced with the increasing imposed rotation. Additionally, the non-dimensional breakup length lies on the line as long as the jets are imposed a same rotating speed and the slope of this characteristic curve decreases as the rotating speed increases.
2. The hysteresis behavior only occurs in larger nozzles, and the JD transition is affected by the imposed rotation, and the critical rotating speed is in linear proportion to flow rate; however, there is no obvious change in DJ transition with the increasing flow rate.
3. Three different breakup patterns can be found depending on the imposed rotation, namely single droplet, satellite droplet, and multi-position necking, respectively. As the rotation speed increases, the multi-positions necking becomes prevailing. Besides, an empirical correlation is proposed for predicting the boundary of satellite and multi-droplets formation.
4. The imposed rotation has slight influence on the breakup droplet size. The sizes of main, satellite, and merged droplets are about 1.8, 0.8, and 2.2 times than the nozzle diameters, respectively, at any rotating speed.
5. Increasing the flow rate of a jet decreases the breakup interval due to the enhancement of inertia forces. The imposed rotation will delay the time interval of a jet owing to the contraction of the breakup length. The non-dimensional time interval between two main droplets has an ascending tendency with either *We* number or the imposed rotation.

ACKNOWLEDGEMENTS

The present study was supported financially by Ministry of Science and Technology, Taiwan under grant number MOST 109-2221-E-006-039.

REFERENCES

Amini, G., M. Ihme and A. Dolatabadi (2013). Effect of gravity on capillary instability of liquid jets. *Physical Review* E 87(5), 053017.

Ashgriz, N. and F. Mashayek (1995). Temporal analysis of capillary jet breakup. *Journal of Fluid Mechanics* 291, 163-190.

Birouk, M. and N. Lekic (2009). Liquid jet breakup in quiescent atmosphere: A review. *Atomization Sprays* 19(6), 501-528.

Bogy, D. (1979). Drop formation in a circular liquid jet. *Annual Review of Fluid Mechanics* 11(1), 207-228.

Bonhoeffer, B., A. Kwade and M. Juhnke (2017). Impact of formulation properties and process parameters on the dispensing and depositioning of drug nanosuspensions using micro-valve technology. *Journal of Pharmaceutical Sciences* 106(4), 1102-1110.

Brandau, T. (2002). Preparation of monodisperse controlled release microcapsules. *International Journal of Pharmaceutics* 242(1-2), 179-184.

Chandrasekhar, S. (1961). *Hydrodynamics and Hydromagnetic Stability*. Oxford: Oxford University Press.

Chemloul, N. S. (2012). Experimental study of cavitation and hydraulic flip effects on liquid jet characteristics into crossflows. *Journal of Applied Fluid Mechanics* 5, 33-43.

Chung, J. M., J. Yoon and Y. Yoon (2015). Effect of recess length on instability in a gas-centered liquid annular jet. *Atomization Sprays* 25(1).

Clanet, C. and J. C. Lasheras (1999). Transition from dripping to jetting. *Journal of Fluid*

Mechanics 383, 307-326.

Eggers, J. and M. P. Brenner (2000). Spinning jets. Paper presented at *the IUTAM Symposium on Nonlinear Waves in Multi-Phase Flow*.

Gao, D. and J. G. Zhou (2019). Designs and applications of electrohydrodynamic 3D printing. *International Journal of Bioprinting* 5(1), 172.

Ghate, K., S. Sharma and T. Sundararajan (2019). Spray atomization characteristics of a low pressure rotary injector. *Atomization Sprays* 29(6).

Gillis, J. (1961). Stability of a column of rotating viscous liquid. Paper presented at the *Mathematical Proceedings of the Cambridge Philosophical Society*.

Grant, R. P. and S. Middleman (1966). Newtonian jet stability. *AIChE Journal* 12(4), 669-678.

Hocking, L. and D. Michael (1959). The stability of a column of rotating liquid. *Mathematika* 6(1), 25-32.

Krištof, O., P. Bulejko and T. Svěrák (2019). Experimental Study on Spray Breakup in Turbulent Atomization Using a Spiral Nozzle. *Processes* 7(12), 911.

Kubitschek, J. and P. Weidman (2007a). The effect of viscosity on the stability of a uniformly rotating liquid column in zero gravity. *Journal of Fluid Mechanics* 572, 261-286.

Kubitschek, J. and P. Weidman (2007b). Helical instability of a rotating viscous liquid jet. *Physics of Fluids* 19(11), 114108.

Labergue, A., M. Gradeck and F. Lemoine (2015). Comparative study of the cooling of a hot temperature surface using sprays and liquid jets. *International Journal of Heat Mass Transfer* 81, 889-900.

Li, Y., G. M. Sisoev and Y. D. Shikhmurzaev (2019). On the breakup of spiralling liquid jets. *Journal of Fluid Mechanics* 862, 364-384.

Lu, Q., R. Muthukumar, H. Ge and S. Parameswaran (2020). Numerical study of a rotating liquid jet impingement cooling system. *International Journal of Heat Mass Transfer* 163, 120446.

McCarthy, M. and N. Molloy (1974). Review of stability of liquid jets and the influence of nozzle design. *The Chemical Engineering Journal* 7(1), 1-20.

Morad, M. R., M. Nasiri and G. Amini (2020). Axis-switching and breakup of rectangular liquid jets. *International Journal of Multiphase Flow* 126, 103242.

Rayleigh, L. (1879). On the capillary phenomena of jets. *Proceedings of the Royal Society of London* 29(196-199), 71-97.

Rutland, D. and G. Jameson (1970). Droplet production by the disintegration of rotating liquid jets. *Chemical Engineering Science* 25(8), 1301-1317.

Savart, F. (1883). Memoire sur la constitution des veines liquides lancees par des orifices circulaires en mince paroi. *Annual Review of Physical Chemistry* 337(53), 337-386.

Son, P. and K. Ohba (1998). Theoretical and experimental investigations on instability of an electrically charged liquid jet. *International Journal of Multiphase Flow* 24(4), 605-615.

Tang, Z., F. Deng, S. Wang and J. Cheng (2021). Numerical Simulation of Flow and Heat Transfer Characteristics of a Liquid Jet Impinging on a Cylindrical Cavity Heat Sink. *Journal of Applied Fluid Mechanics* 14(3), 723-732.

Utreja, L. and D. Harmon (1990). *Aerodynamic breakup of liquid jets-A review.* Paper presented at the 21st Fluid Dynamics, Plasma Dynamics and Lasers Conference.

Wang, F. and T. Fang (2015). Liquid jet breakup for non-circular orifices under low pressures. *International Journal of Multiphase Flow* 72, 248-262.

Wang, Y. b., J. P. Guo, F. Q. Bai and Q. Du (2018). Influences of bounded and compressible gas medium on the instability of an annular power-law liquid jet. *Atomization Sprays* 28(5).

Weidman, P., J. Kubitschek and A. Medina (2008). Profiles of flow discharged from vertical rotating pipes: A contrast between inviscid liquid and granular jets. *Physics of Fluids* 20(11), 117101.

Yang, L. J., T. Hu, P. M. Chen and H. Y. Ye (2017). Nonlinear spatial instability of a slender viscous jet. *Atomization Sprays* 27(12).

Zahniser, R. (2004). *Instabilities of rotating jets.* (B.S. thesis), Massachusetts Institute of Technology, Boston.